

RESEARCH ARTICLE

[View Article Online](#)
[View Journal](#) | [View Issue](#)



Cite this: *Inorg. Chem. Front.*, 2021, 8, 3085

A facile fabrication of a multi-functional and hierarchical Zn-based MOF as an efficient catalyst for CO₂ fixation at room-temperature

Jianwen Lan, Ye Qu, Zhijiang Wang, Ping Xu and Jianmin Sun *

Carboxyl-containing and amine-rich Zn-MOF [Zn₂L₂MA-2DMF] (MA = melamine, H₂L = 2,5-thiophenedicarboxylic acid) was facilely synthesized by a simple room-temperature stirring approach. In addition, the synthesis period was reduced to 2 h due to the organic amine of triethylamine (TEA), tripropylamine (TPA) or triamylamine (TAA) as a protonation agent, which made the fabrication of Zn-MOF both time- and energy-saving. The obtained Zn-MOF possessed hierarchical pores (labeled as Hie-Zn-MOF) and efficiently catalyzed the CO₂ fixation with epoxides. The existing mesopores in Hie-Zn-MOF were beneficial for the diffusion and accessibility of substrates as well as the carbonate product, while the micropores accelerated CO₂ gathering and strengthened its interaction with active sites. Hie-Zn-MOF-TEA with TEA as a protonation agent exhibited 97% yield of propene carbonate at room temperature. In particular, the catalytic activity for bulky epoxides was evidently higher than that for comparative Zn-MOF with only micropores (labeled as Mic-Zn-MOF), and the corresponding product yield was obviously improved from 64% to 88% with the butyl glycidyl ether substrate. Besides, the tentative synthesis procedure for the Hie-Zn-MOF catalyst and the feasible catalytic mechanism for CO₂ fixation to epoxides are proposed. The time- and energy-saving synthesis strategy and efficient Zn-MOF catalyst are attractive in CO₂ capture and CO₂ chemical conversion.

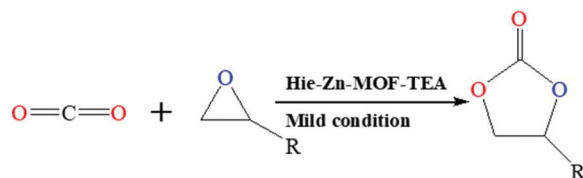
Received 26th January 2021,
Accepted 29th April 2021

DOI: 10.1039/d1qi00104c
rsc.li/frontiers-inorganic

Introduction

Climate change caused by the rapid increase in the atmospheric carbon dioxide concentration from anthropogenic activities, particularly fossil fuel combustion, is a global environmental crisis. Significant efforts have been devoted to CO₂ capture, storage and utilization.¹ Moreover, CO₂ chemical fixation is widely pursued as a hot topic because CO₂ is non-toxic, abundant and renewable C1 feed-stock for the synthesis of valuable chemicals.² One of the most effective and promising strategy is the CO₂ cycloaddition with epoxides to generate cyclic carbonate (Scheme 1), which is a highly atom-economical reaction with minimal by-products,³ the products of cyclic carbonates are widely applied as electrolytes in lithium-ion batteries, aprotic solvents and valuable precursors for medicine and polymer synthesis.⁴ Thus, massive efforts are focused on the development of efficient catalysts to facilitate the CO₂ cycloaddition to numerous epoxides.⁵

In the past decades, metal organic frameworks (MOFs) have been developed for CO₂ capture and catalysis owing to their composition tenability, unique structure, high surface area and porosity.⁶ However, most reported MOFs were microporous materials, which seriously limit the substrate diffusion and transfer, particularly for bulky molecule reagents.⁷ The existence of mesopores is anticipated to improve catalytic activity; however, only a few mesoporous MOF catalysts have been developed for CO₂ fixation due to their collapsible and perforative nature.⁸ Therefore, hierarchical MOFs with micropores and mesopores perfectly overcame the shortcomings of single microporous or mesoporous MOFs.^{9–11} For example, hierarchical porous MOF-5-MIX achieved 93% product yield for the CO₂ cycloaddition to propylene oxide under the con-



State Key Laboratory of Urban Water Resource and Environment, MIIT Key Laboratory of Critical Materials Technology for New Energy Conversion and Storage, School of Chemistry and Chemical Engineering, Harbin Institute of Technology, Harbin 150080, China. E-mail: sunjm@hit.edu.cn

Scheme 1 Hie-Zn-MOF-TEA catalyzing the CO₂ cycloaddition with epoxides.

ditions of 50 °C, 1.2 MPa and 5 h.¹² Similarly, for hierarchical UCMC-1-NH₂, the propylene carbonate yield was up to 90% with prolonged reaction time 24 h at room temperature.¹³ Moreover, MOFs are usually synthesized by a solvothermal method at high temperatures and long synthesis period.¹⁴ It was also reported that few typical MOFs such as ZIF-8¹⁵ and ZIF-67¹⁶ could be prepared by simple agitation at room temperature, but a high ligand/metal ion ratio was required, which inevitably resulted in the excessive addition of ligand amounts. Furthermore, the room-temperature synthesis of MOFs with mixed-ligands was rarely studied due to its complicated self-assembly process. Hence, the rapid synthesis of MOF catalysts with mixed ligands particularly at room temperature is still necessary for the development of efficient catalyst candidates for CO₂ cycloaddition.

Herein, a hierarchical Zn-based MOF (Hie-Zn-MOF) was facilely achieved by simple stirring at room-temperature for 2 h using an organic amine as a protonation agent, which was more facile and energy-saving compared to the solvothermal synthesis. Hie-Zn-MOF with different organic amine loadings was characterized thoroughly. Due to the concomitant micropores and formative mesopores, Hie-Zn-MOF-TEA showed a good CO₂ adsorption capacity of 84.9 cm³ g⁻¹ at 273 K and high catalytic activity for the CO₂ cycloaddition reaction with epoxides. Particularly for bulky epoxides, such as a butyl glycidyl ether substrate, the corresponding product yield obviously improved from 64% to 88% compared with a pure Mic-Zn-

MOF catalyst by the solvothermal synthesis. The high recyclability and good generality to other substrates of the Hie-Zn-MOF-TEA catalyst were also verified. Besides, the feasible synthesis procedure and catalytic mechanism of Hie-Zn-MOF for CO₂ cycloaddition to epoxide were further proposed. The developed efficient Zn-based MOF catalyst with a hierarchical structure and its facile room-temperature synthesis are highly attractive in CO₂ capture and utilization.

Results and discussion

Hie-Zn-MOF characterizations

Gas sorption properties. For investigating the porous nature of Mic-Zn-MOF and several Hie-Zn-MOF samples, N₂ adsorption–desorption measurements were conducted. In Fig. 1A and C, all N₂ sorption curves were characterized by a sharp rise within a low relative pressure ($P/P_0 < 0.01$), demonstrating the existence of micropores. For Hie-Zn-MOF samples, the typical IV sorption isotherms with obvious hysteresis loops were also observed within $0.4 < P/P_0 < 1$, suggesting the presence of a mesoporous structure.^{12,18} The N₂ adsorption–desorption isotherm of Mic-Zn-MOF synthesized by the solvothermal method was attributed to the type I behavior, which confirmed its microporous nature.¹⁹ Further pore size distribution was calculated based on adsorption branches (Fig. 1B); Hie-Zn-MOF with TEA addition (Hie-Zn-MOF-TEA) presented distinct meso-

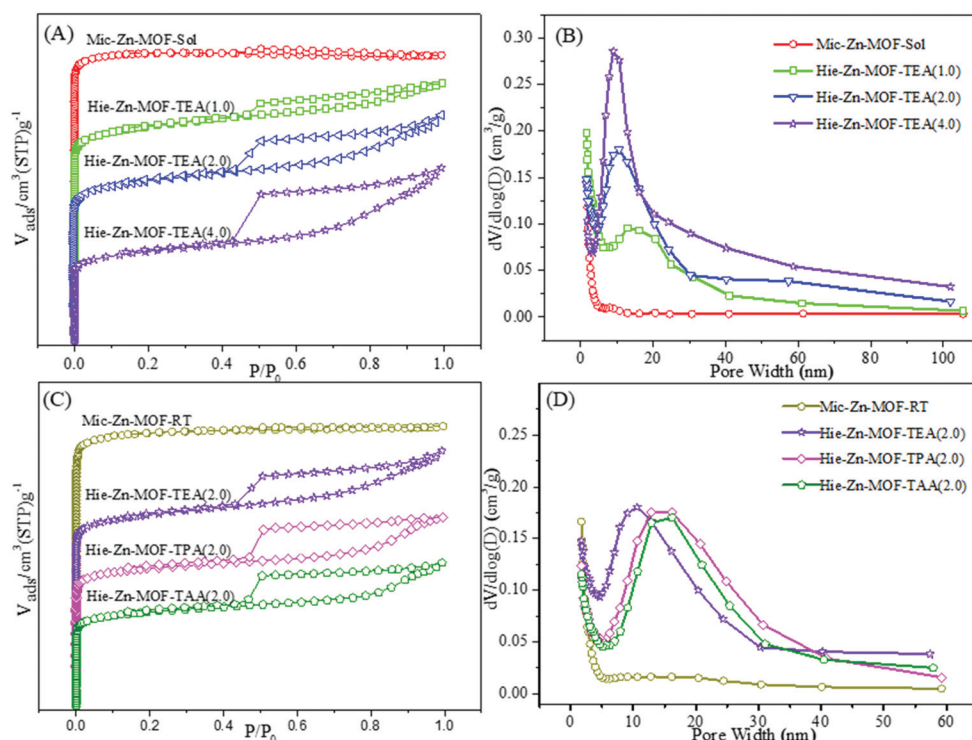


Fig. 1 (A) N₂ adsorption–desorption isotherms, the isotherms for Mic-Zn-MOF-Sol, Hie-Zn-MOF-TEA(1.0) and Hie-Zn-MOF-TEA(2.0) are offset by 150, 100 and 50 cm³ g⁻¹, respectively, for clarity (B) relative pore size distributions (C) N₂ adsorption–desorption isotherms, the isotherms for Mic-Zn-MOF-RT, Hie-Zn-MOF-TEA(2.0) and Hie-Zn-MOF-TPA(2.0) are offset by 150, 100 and 50 cm³ g⁻¹, respectively, (D) relative pore size distributions.

Table 1 Porosity structure and CO₂ uptake of Hie-Zn-MOF

Porous MOF	S_{BET} (m ² g ⁻¹)	V_{micro} (cm ³ g ⁻¹)	V_{meso} (cm ³ g ⁻¹)	CO ₂ uptake (cm ³ g ⁻¹)	
				273 K	298 K
Mic-Zn-MOF-Sol	1006	0.392	—	108.9	79.7
Mic-Zn-MOF-RT	841	0.391	—	94.1	62.3
Hie-Zn-MOF-TEA(1.0)	711	0.247	0.149	84.9	55.4
Hie-Zn-MOF-TEA(2.0)	625	0.211	0.185	73.2	44.0
Hie-Zn-MOF-TEA(4.0)	528	0.178	0.219	50.4	34.1
Hie-Zn-MOF-TPA(2.0)	534	0.189	0.169	53.3	34.5
Hie-Zn-MOF-TAA(2.0)	494	0.174	0.145	44.4	30.8

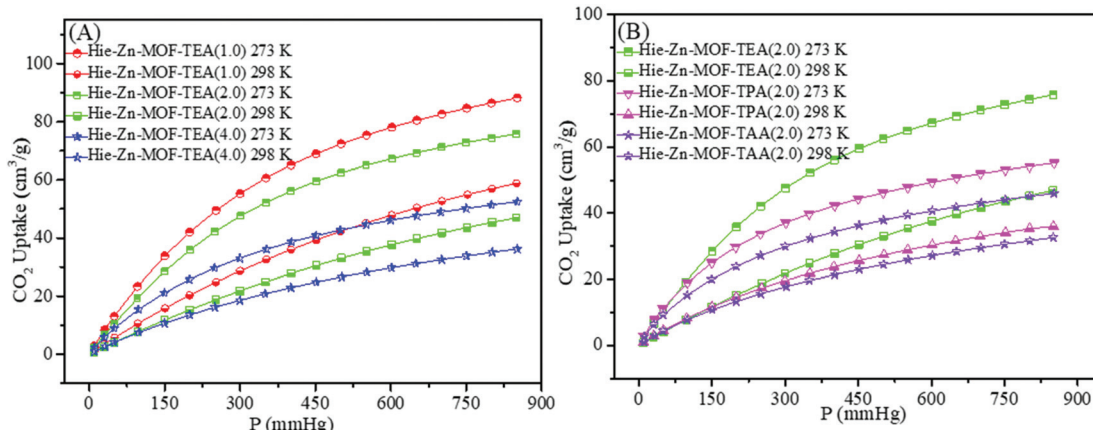
pores ranging from 5–30 nm compared with Mic-Zn-MOF-Sol. By using an organic amine with a longer chain length such as TPA or TAA, Hie-Zn-MOF-TPA(2.0) and Hie-Zn-MOF-TAA(2.0) samples showed wider distributions of the pore diameter (Fig. 1D). Detailed porosity data are summarized in Table 1; compared with the high surface area at 1006 m² g⁻¹ of Mic-Zn-MOF-Sol (microporous Zn-MOF prepared by the solvothermal synthesis, in catalyst synthesis section), the BET surface area of Mic-Zn-MOF-RT (microporous Zn-MOF prepared without organic amines, in the catalyst synthesis section) powders was reduced to 841 m² g⁻¹ due to the partial destruction of the porous framework resulting from vigorous room-temperature stirring. The surface area of hierarchical Hie-Zn-MOF samples further declined because of the reduction of the microporous structure. With TEA loading increasing from 1.0 to 4.0 mmol, the BET surface areas of Hie-Zn-MOF-TEA(1.0), Hie-Zn-MOF-TEA(2.0), Hie-Zn-MOF-TEA(4.0) were calculated to be 711, 625 and 528 m² g⁻¹, respectively. Moreover, their mesopore volume rose to 0.219 cm³ g⁻¹ for Hie-Zn-MOF-TEA(4.0). Also, Hie-Zn-MOF-TPA(2.0) and Hie-Zn-MOF-TAA(2.0) possessed mesoporous structures and high surface areas at 534 and 494 m² g⁻¹, respectively. The systematic N₂ sorption analysis confirmed the existence of hierarchical structures in several Hie-Zn-MOF samples. The existence of mesopores in Hie-Zn-MOF facilitated substrates transfer and micropores accelerated

CO₂ gathering, which were beneficial to the improvement of catalytic CO₂ cycloaddition performance.²⁰

The high CO₂ sorption capacity revealed positive influence on the catalytic performance of porous materials over CO₂ chemical fixation,²¹ which urged us to further investigate the potential of Hie-Zn-MOF samples for CO₂ capture. The CO₂ adsorptive values were respectively collected at 273 K and 298 K, as shown in Fig. 2A. The CO₂ uptake values of Hie-Zn-MOF-TEA samples decreased with the reduction of their surface areas and was respectively calculated to be 84.9 cm³ g⁻¹, 73.2 cm³ g⁻¹, 50.4 cm³ g⁻¹ for Hie-Zn-MOF-TEA(1.0), Hie-Zn-MOF-TEA(2.0), Hie-Zn-MOF-TEA(4.0) at 273 K. Hie-Zn-MOF-TPA(2.0) and Hie-Zn-MOF-TAA(2.0) showed the CO₂ uptake at 53.3 and 44.4 cm³ g⁻¹ at 273 K. The Mic-Zn-MOF-Sol sample showed the highest CO₂ adsorption capacity of 108.9 cm³ g⁻¹ because the microporous structure afforded the highest surface area and more adsorption sites in the case of the similar pore volume. Moreover, the corresponding adsorption heat Q_{st} of Hie-Zn-MOF was ranging from 23.5 to 27.8 kJ mol⁻¹, which revealed appropriate interactions between the Hie-Zn-MOF framework and CO₂ molecules, facilitating CO₂ easy desorption and adsorbent regeneration.²²

Powder XRD and FT-IR characterizations. The high crystallinity and distinct structural information of Hie-Zn-MOF samples were confirmed by the sharp and clear diffraction peaks in PXRD patterns (Fig. 3A), and most peaks were in good agreement with the patterns of Mic-Zn-MOF-Sol, testifying the similarity of the Hie-Zn-MOF structure with Mic-Zn-MOF-Sol. Moreover, the PXRD pattern of Mic-Zn-MOF-RT matched well with Mic-Zn-MOF-Sol and proved the successful synthesis of Mic-Zn-MOF at room temperature (Fig. 3B). FT-IR characterization for Hie-Zn-MOF-TEA and Mic-Zn-MOF samples was carried out to verify their constituents and functional groups. As shown in Fig. 4, most characteristic peaks of Hie-Zn-MOF-TEA were completely consistent with the Mic-Zn-MOF crystal synthesized by the solvothermal synthesis, demonstrating their similar compositions.

The peak at 3401 cm⁻¹ was attributed to the stretching vibrations of N-H from the MA ligand.¹⁷ The broad peak at

**Fig. 2** CO₂ adsorption isotherms of (A) Hie-Zn-MOF-TEA (B) Hie-Zn-MOF-TPA and Hie-Zn-MOF-TAA.

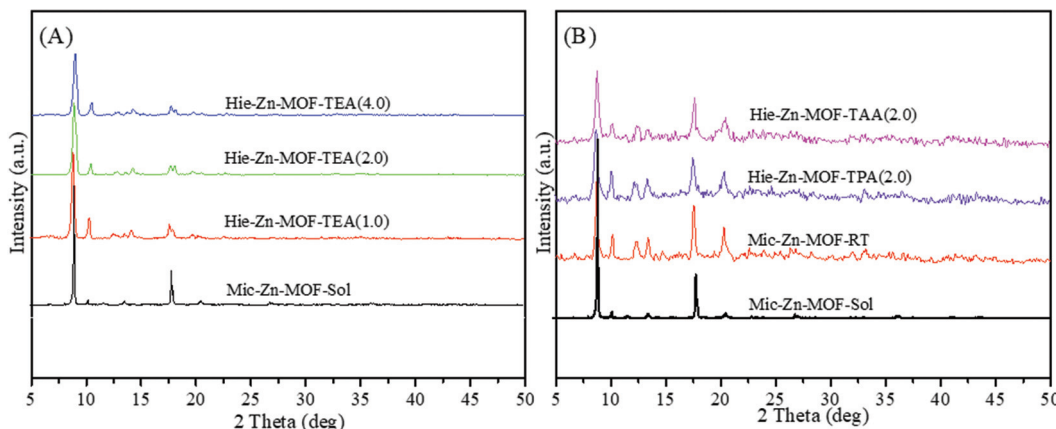


Fig. 3 (A) XRD patterns of Hie-Zn-MOF-TEA and (B) Hie-Zn-MOF-TPA and Hie-Zn-MOF-TAA.

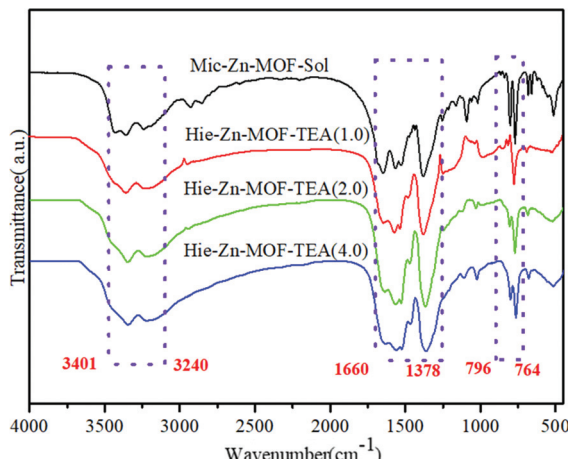


Fig. 4 FT-IR spectra of Hie-Zn-MOF-TEA and Mic-Zn-MOF.

3240 cm^{-1} and strong peak at 1660 cm^{-1} were assigned to O-H and C=O stretching vibrations, and the carboxylate asymmetric stretching vibration and bending vibration mode at 1378 cm^{-1} and 796 cm^{-1} indicated the presence of carboxyl groups.²³ Besides, the band located at 522 cm^{-1} was due to Zn-O stretching vibrations.²⁴

XPS and ICP analyses. The chemical states of the elements were identified via XPS. In Fig. 5A, the XPS survey scans of Hie-Zn-MOF-TEA(4.0) verified the existence of Zn, O, N, C and S elements. For the Zn 2p spectrum, the two peaks at 1021.8 and 1044.9 eV were assigned to Zn 2p_{3/2} and 2p_{1/2}, respectively.²⁵ The C 1s spectra in Fig. 5C were deconvoluted into four peaks at 284.6, 286.1, 288.3 and 290.2 eV, which are assigned to C-C, C-N, O=C-O, and C=N bonds, respectively.²⁶ In Fig. 5D, the O 1s spectra of Hie-Zn-MOF-TEA(4.0) revealed three peaks located at 531.4, 533.0, and 534.3 eV attributed to C-O, Zn-O and C=O bonds, respectively.²⁷ Besides, the ICP analysis showed that the Zn content of Hie-Zn-MOF-TEA(4.0) was about 18.3 wt%, similar to 17.7 wt% of the Mic-Zn-MOF-Sol crystal in our previous report.¹⁷

The SEM image of Mic-Zn-MOF-Sol is shown in Fig. 6A, and shows that the Mic-Zn-MOF-Sol has a cubic crystal structure. The SEM and TEM images of Hie-Zn-MOF-TEA(4.0) indicated that the sample had submicron aggregation or packing of massive Zn-MOF sheets and its size was 100–200 nm. The decrease in the size compared with Mic-Zn-MOF-Sol was attributed to the high nucleation rate and TEA as capping agents, preventing the further growth of Zn-MOF microcrystals.²⁸ Besides, mesopores are observed in Fig. 6C, and the EDS mapping showed a good distribution of Zn, O, N, C and S elements. Based on the pioneering reported research and above experiment result, a feasible synthesis procedure for Hie-Zn-MOF was proposed. As illustrated in Scheme 2, the organic amine of TEA as a protonation agent made the deprotonation of the ligands to happen promptly, which was considered as the key step for the MOF rapid assembly.^{29,30} Furthermore, free Zn²⁺ ions connected to deprotonated ligands with the aid of continuous stirring, while the binding of TEA molecules to metal ions in competition with the deprotonated ligands prevented the further growth of Zn-MOF microcrystals.^{29,31} Besides, numerous TEA⁺ ions were enriched and stored in the framework due to their electrostatic interactions with deprotonated ligands.³² Finally, after a simple convenient solvent washing and vacuum drying process, mesopores were generated from the removal of numerous TEA molecules, forming mesopores in Zn-MOF.³³

Catalytic CO₂ cycloaddition reaction with epoxides

The high CO₂ adsorption capacity of several Hie-Zn-MOF samples encouraged us to explore their catalytic activity for the CO₂ cycloaddition to epoxides. As shown in Table 2, in the presence of the Bu₄NBr co-catalyst, Hie-Zn-MOF-TEA, Hie-Zn-MOF-TPA, Hie-Zn-MOF-TAA all showed over 95% propylene carbonate (PC) yield within 2.5 h, which was comparable to Mic-Zn-MOF with the highest surface area under the same reaction conditions (entries 1–5). Among the several Hie-Zn-MOF catalysts, Hie-Zn-MOF-TEA(4.0) presented the most

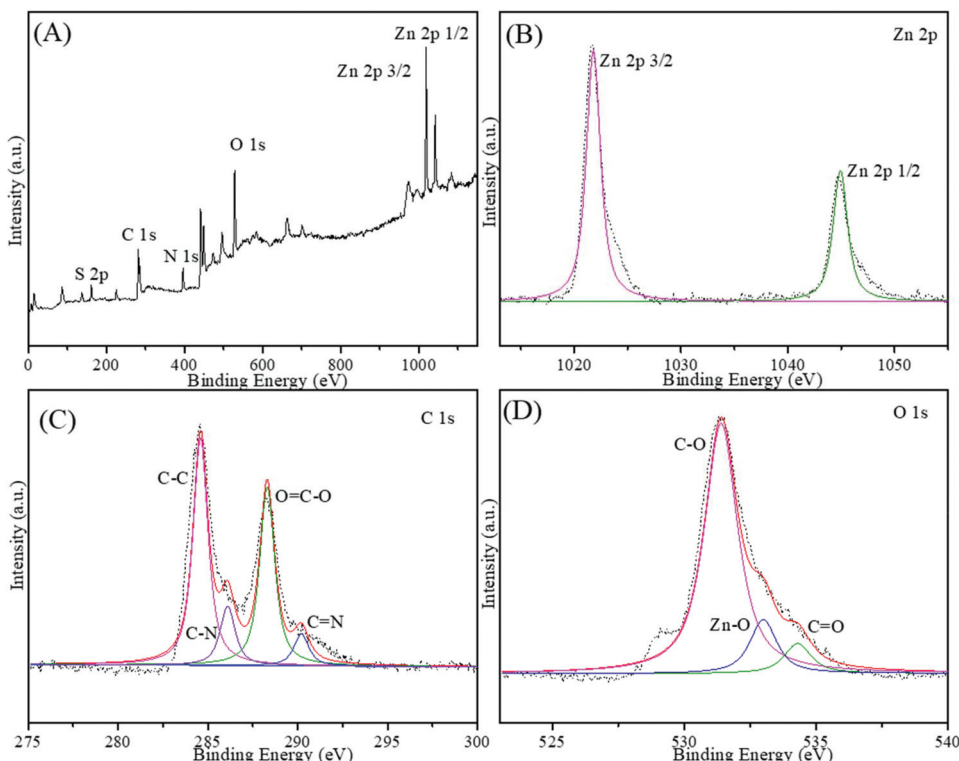


Fig. 5 XPS spectra of Hie-Zn-MOF-TEA(4.0): (A) survey spectrum and (B) Zn 2p, (C) C 1s, (D) O 1s spectra.

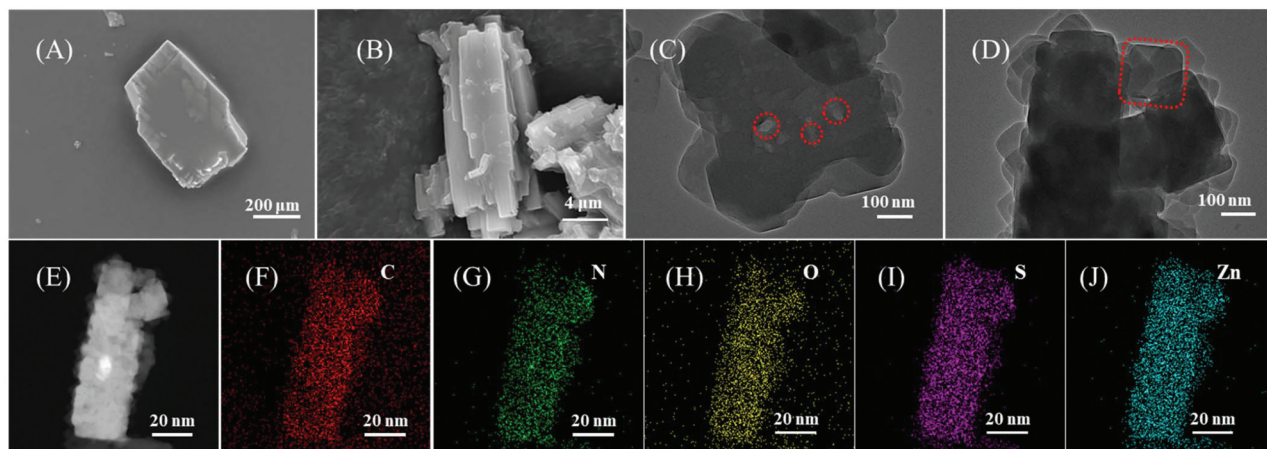
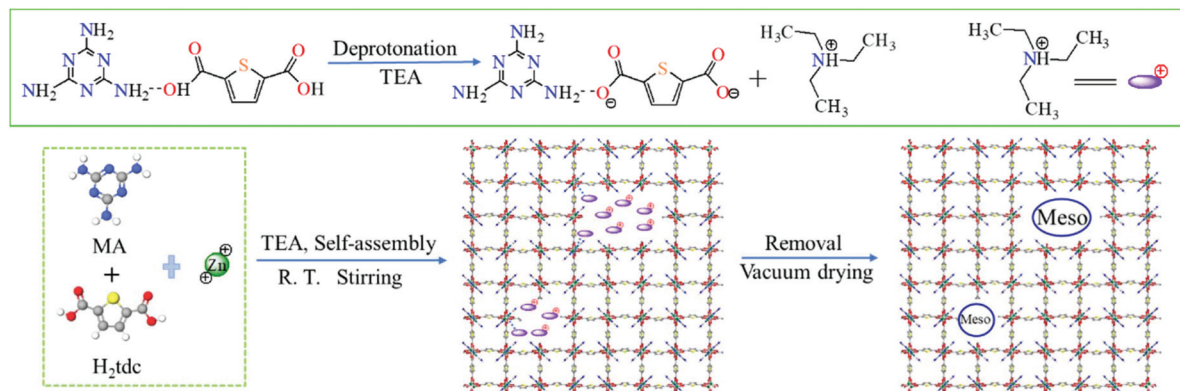


Fig. 6 SEM images of (A) Mic-Zn-MOF-Sol, (B) Hie-Zn-MOF-TEA(4.0) sample, (C) (D) (E) TEM images of Hie-Zn-MOF-TEA(4.0) sample, (F–J) Energy dispersive spectroscopy (EDS) elemental mappings of Hie-Zn-MOF-TEA(4.0) sample for C, N, O, S and Zn.

efficient catalytic activity due to its highest mesopore volume and 97% PC yield was obtained under the conditions of room temperature, 1 MPa CO₂ and 16 h (entries 6–9). Compared with Mic-Zn-MOF (entry 6), the reaction time was further reduced as a result of the synergistic effects of micro- and mesopores. The advantage of mesopores encouraged us further explore the catalytic performance for bulky epoxides. Under room temperature, the enhancement of the catalytic performance of Hie-Zn-MOF-TEA(4.0) was not satisfactory

enough due to fewer effective collisions (entries 10–13). While there are obvious increase in the product yield at 80 °C, however for butyl glycidyl ether (BGE) of bulky epoxide as a substrate, Mic-Zn-MOF/Bu₄NBr catalysts presented 64% product yield under the mild conditions of 80 °C, 1 MPa CO₂ pressure and 3 h (entry 14). The target product yield increased remarkably over Hie-Zn-MOF catalysts and up to 88% was obtained over Hie-Zn-MOF-TEA(4.0)/Bu₄NBr catalysts (entries 15–19). The enhancement in the catalytic performance of Hie-



Scheme 2 Feasible synthesis procedure of Hie-Zn-MOF.

Table 2 Catalytic performance of several Hie-Zn-MOF under mild conditions

Entry	Catalyst	Epoxide	Time (h)	Tem. (°C)	Yield (%)	Sel. (%)
1	Mic-Zn-MOF	PO	3	80	99	>99
2	Hie-Zn-MOF-TEA(2.0)	PO	2.5	80	98	>99
3	Hie-Zn-MOF-TPA(2.0)	PO	2.5	80	96	>99
4	Hie-Zn-MOF-TAA(2.0)	PO	2.5	80	95	>99
5	Hie-Zn-MOF-TEA(4.0)	PO	2.5	80	96	>99
6	Mic-Zn-MOF ^a	PO	24	25	98	98
7	Hie-Zn-MOF-TEA(1.0) ^a	PO	16	25	90	97
8	Hie-Zn-MOF-TEA(2.0) ^a	PO	16	25	92	98
9	Hie-Zn-MOF-TEA(4.0) ^a	PO	16	25	97	98
10	Mic-Zn-MOF ^a	BGE	16	25	62	98
11	Hie-Zn-MOF-TEA(4.0) ^a	BGE	16	25	74	98
12	Mic-Zn-MOF ^a	SO	24	25	54	96
13	Hie-Zn-MOF-TEA(4.0) ^a	SO	24	25	62	95
14	Mic-Zn-MOF	BGE	3	80	64	96
15	Hie-Zn-MOF-TEA(1.0)	BGE	3	80	80	96
16	Hie-Zn-MOF-TEA(2.0)	BGE	3	80	81	97
17	Hie-Zn-MOF-TEA(4.0)	BGE	3	80	88	97
18	Hie-Zn-MOF-TPA(2.0)	BGE	3	80	82	96
19	Hie-Zn-MOF-TAA(2.0)	BGE	3	80	80	97

Reaction conditions: Zn-MOF catalyst 0.1 g, co-catalyst Bu_4NBr 0.1 g, epoxide 34.5 mmol, CO_2 pressure 1.0 MPa; PO, propylene oxide, BGE (butyl glycidyl ether). Product yield and selectivity were determined by the GC analysis. ^a Bu_4NBr 0.25 g, the other conditions are the same.

Zn-MOF was attributed to the formed mesopore structures, which facilitated the diffusion process of the substrate and corresponding product.

CO_2 cycloaddition to numerous epoxides over the Hie-Zn-MOF catalyst

Epoxides with different substituents were applied to investigate the catalytic versatility of Hie-Zn-MOF-TEA(4.0)/ Bu_4NBr catalysts under the reaction conditions of 80 °C, 1 MPa CO_2 and 3 h (Fig. 7). For the small epoxides of propylene oxide (PO) and 1,2-epoxybutane (BO), the corresponding product yields were above 98%, comparable to the Mic-Zn-MOF catalyst. With Hie-Zn-MOF-TEA(4.0)/ Bu_4NBr catalysts, the product yield of epichlorohydrin (ECH) was improved to 86% from 63% over the Mic-Zn-MOF catalyst. Attractively, with bulky epoxide as a

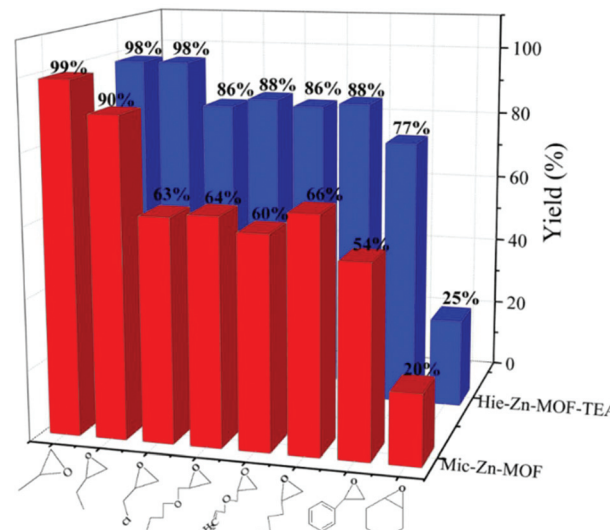


Fig. 7 Versatility of the Hie-Zn-MOF-TEA(4.0)/ Bu_4NBr catalyst. Reaction conditions: epoxide 34.5 mmol, Zn-MOF catalyst 0.1 g, Bu_4NBr 0.1 g, 80 °C, 1 MPa CO_2 , 3 h.

reactant, such as butyl glycidyl ether (BGE), allyl glycidyl ether (AGE), 1,2-epoxyhexane (EH), high product yields (>86%) were achieved under the same conditions, and comparatively, only medium yields were obtained over the Mic-Zn-MOF catalyst. Similarly, Hie-Zn-MOF-TEA(4.0) exhibited positive catalytic performance to bulky styrene oxide (SO) with the product yield at 77%. The significantly enhanced activity to the bulky epoxides over the Hie-Zn-MOF catalyst was because the mesopores of the Hie-Zn-MOF-TEA(4.0) catalyst afforded a free path for the bulky epoxides to access the plentiful internal active sites, which significantly favored their catalytic performance.³⁴ For cyclohexane oxide (CHO), with the high steric hindrance of the cyclohexane ring, only 25% corresponding carbonate yield was obtained. Moreover, the good catalytic performances for bulky epoxides (AGE or BGE) of the Hie-Zn-MOF-TEA(4.0)/ Bu_4NBr system were superior to most microporous MOFs due to the existence of mesopores. Besides, it showed 86% product yield

for AGE under mild conditions and 97% PC yield at room temperature, which was superior or comparable to the reported hierarchical MOFs (Table 3).

Recyclability of the Hie-Zn-MOF catalyst

For an efficient heterogeneous catalyst, besides high catalytic activity, the recyclability is also a decisive criterion for potential industrial applications. After each run, the reused Hie-Zn-MOF-TEA(4.0) catalyst was easily separated by simple centrifugation, then washed, and dried for next run. Under the reac-

tion conditions of 80 °C, 1 MPa CO₂ and 3 h, the regeneration for catalyzing the CO₂ cycloaddition with PO was explored. As illustrated in Fig. 8A, Hie-Zn-MOF-TEA(4.0) exhibited excellent recyclability and could be continuously reused for 5 runs, maintaining high catalytic activity. Correspondingly, the peak locations of XRD patterns and XPS survey scan of the reused Hie-Zn-MOF-TEA(4.0) catalyst were also consistent with that of the fresh sample (Fig. 8C and D), which further confirmed its high stability during the consecutive cycloaddition reactions. The declined peak intensities of XRD were a result of the

Table 3 Comparisons of Hie-Zn-MOF-TEA/Bu₄NBr catalysts with numerous MOF catalysts in previous reports

Catalyst	Epoxide	Time (h)	Tem. (°C)	Press. (MPa)	Yield (%)	Ref.
Microporous MOFs	Mn-BTC	AGE	9	105	88	35
	[Zn ₈ (Ad) ₄ (DABA) ₆ O]	AGE	24	100	74	36
	NH ₂ -MIL-125	AGE	2	100	68	37
	Cu(Hip) ₂ (Bpy)	AGE	6	80	89	38
	PNU-22	AGE	8	80	75	39
	Zn(Bmic)(AT)	BGE	6	80	51	40
Hierarchical MOFs	Hie-Zn-MOF-TEA	PO	16	r.t.	97	This work
		AGE	3	80	86	This work
	UMCM-1-NH ₂	PO	24	r.t.	90	12
		AGE	24	r.t.	55	12
	MOF-5-MIX	PO	6	50	93	13
		AGE	6	50	83	13
	HP-MIL-88-NH ₂ (Fe)	PO	12	45	94	41
		AGE	12	45	72	41
	MOF-74-III	PO	48	r.t.	98	42

Reaction substrate: PO, propylene oxide; BGE, butyl glycidyl ether; AGE, allyl glycidyl ether; r.t. = room temperature.

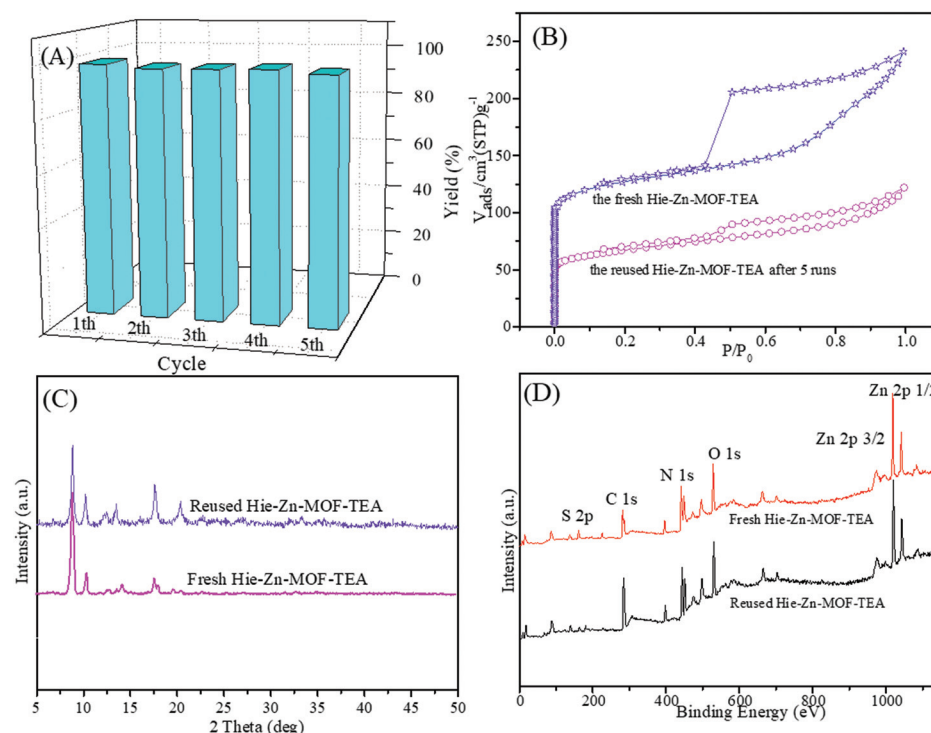


Fig. 8 (A) Recyclability and (B) N₂ adsorption–desorption isotherm (C) XRD patterns (D) XPS spectra for fresh and reused Hie-Zn-MOF-TEA(4.0) catalyst after 5 runs.

decrease in crystallinity after recycling. Moreover, further ICP analysis on the reused Hie-Zn-MOF-TEA(4.0) catalysts showed that the Zn content was about 17.8wt%, which was similar to 18.3wt% of the fresh one, which might slightly affect the recyclability of the Hie-Zn-MOF-TEA(4.0) catalyst. Moreover, the N_2 adsorption–desorption isotherm of the reused Hie-Zn-MOF-TEA(4.0) catalyst (Fig. 8B) also showed typical IV sorption isotherms with obvious hysteresis loops, while the BET surface area was decreased from $528\text{ m}^2\text{ g}^{-1}$ to $240\text{ m}^2\text{ g}^{-1}$ after 5 runs, which was ascribed to partial blockage of the porous structure by the residual product of propylene carbonate.

Feasible mechanism for CO_2 cycloaddition with epoxide over Hie-Zn-MOF

Previous theoretical studies revealed that hierarchical pores could afford numerous available active sites and facilitate the mass transfer process of substrates.⁴³ In addition, the synergistic effects of Lewis acid and base sites were critical for the cycloaddition reaction of epoxides and CO_2 .¹ The Zn coordination environments of the Hie-Zn-MOF catalyst is shown in Fig. 9A, and the distance between Zn sites and $-\text{NH}_2$ sites was 3.12 \AA , which was beneficial to enhance their synergistic effects for catalytic reactions.³⁶ On this basis, a possible reaction mechanism is presented in Scheme 3. Substrates of CO_2

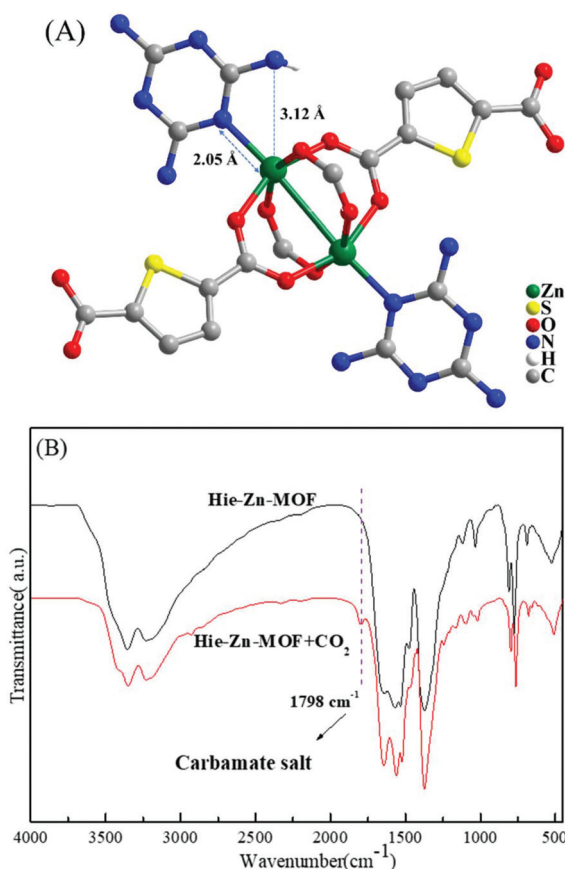
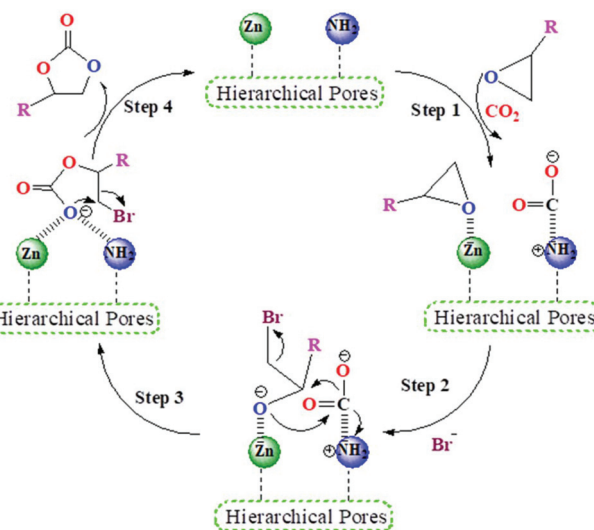


Fig. 9 (A) Zn coordination environment in Hie-Zn-MOF (B) FT-IR spectra of fresh and CO_2 activated Hie-Zn-MOF at $80\text{ }^\circ\text{C}$, 1 MPa for 3 h .



Scheme 3 Plausible reaction mechanism for the CO_2 cycloaddition to epoxide catalyzed by Hie-Zn-MOF/ Bu_4NBr .

and epoxides were highly enriched and dispersed into hierarchical pores, which then accessed to active sites. Zn sites and $-\text{NH}_2$ groups in Hie-Zn-MOF as Lewis acid–base sites activated epoxides and CO_2 molecules by the formation of a Zn–O adduct and carbamate salt (step 1), which was affirmed by the new peak in the FT-IR spectra at 1798 cm^{-1} (in Fig. 9B).⁴⁴ Simultaneously, the ring-opening occurred smoothly with the help of a nucleophilic attack of Br^- anions of the Bu_4NBr cocatalyst to the β -carbon atom of epoxide (step 2). Then, the intermediate of ring-opened epoxide interacted with the activated carbamate salt to form an alkylcarbonate anion (Step 3), which was converted to the corresponding cyclic carbonate with the occurrence of a ring-closure reaction and regeneration of the Hie-Zn-MOF catalyst (Step 4). The existing mesopores in Hie-Zn-MOF were beneficial for the diffusion and accessibility of substrates and carbonate product, while the micropores accelerated CO_2 gathering and strengthened its interactions with active sites. Therefore, Hie-Zn-MOF exhibited a high yield of 97% to propene carbonate at room temperature, particularly remarkable yield improvement was exhibited with the bulky epoxide as the substrate.

Conclusion

Carboxyl-containing and amine-rich Zn-based MOF was facilely synthesized from mixed ligands of melamine and 2,5-thiophenedicarboxylic acid by room-temperature stirring for 1 week; however, the synthesis process was remarkably reduced to 2 h by employing organic amines of TEA, TPA or TAA to facilitate the deprotonation of the ligands. The present room-temperature stirring synthesis for Zn-MOF was highly efficient and energy-saving compared with the traditional solvothermal method. Besides, mesopores ranging from 5 to 30 nm were generated in Zn-MOF materials to obtain the hierarchical

pores (Hie-Zn-MOF). Due to the concomitant micropores and high surface area, Hie-Zn-MOF-TEA synthesized using TEA as a protonation agent showed a high CO₂ adsorption capacity of 84.9 cm³ g⁻¹ at 273 K and catalytic activity for the CO₂ cycloaddition with epoxide, and 97% propylene carbonate yield was achieved under the conditions of room temperature, 1 MPa and 16 h. Particularly for the bulky epoxides, the corresponding cyclic carbonate yield evidently improved compared with that of the Mic-Zn-MOF synthesized by the solvothermal method, which was a result of the existing mesopores in Hie-Zn-MOF, contributing to the free path for the diffusion and accessibility of substrates and carbonate products. The high recyclability and good tolerance to other epoxides were also affirmed. Besides, the feasible procedures for the Hie-Zn-MOF synthesis and catalytic CO₂ cycloaddition mechanism were proposed. The time- and energy-saving synthesis strategy of an efficient Zn-based MOF catalyst with the hierarchical structure is of great potential in CO₂ capture and utilization.

Experimental section

Characterization

The FT-IR analysis was conducted on a Spectrum 100 Spectrometer (PerkinElmer) with the range of 4000–450 cm⁻¹. Powder X-ray diffraction (PXRD) spectra were recorded using a Bruker D8 Advance X-ray diffractometer with a step size of 0.05°. Gas adsorption tests were performed on Micromeritics ASAP2020 after the conventional degassing process at 150 °C for 8 h. Brunauer–Emmett–Teller (BET) surface area was obtained based on the N₂ adsorption–desorption isotherm and corresponding pore size distribution was obtained using adsorption branch. Inductively coupled plasma (ICP Optima 8300, PerkinElmer) measurements were obtained to determine the Zn²⁺ concentration. X-ray photoelectron spectroscopy (XPS) was conducted on Thermo Fisher Scientific Escalab 250Xi. CO₂ sorption isotherms were collected at 298 K and 273 K, respectively. A scanning electron microscope (SEM, TM3030plus, Hitachi, Japan) and transmission Electron Microscope (TEM, Tecnai G2 Spirit electron microscope) were used to observe the surface morphology. Gas chromatography (GC) was performed by Agilent GC-7890A with an autosampler.

Synthesis of Hie-Zn-MOF

Typically, a mixture of 1 mmol Zn(NO₃)₂·6H₂O (0.297 g), 1 mmol 2,5-thiophenedicarboxylic acid (H₂L, 0.172 g) and 0.66 mmol melamine (MA, 0.084 g) was completely dissolved in 40 mL *N,N*-dimethylformamide (DMF); different amounts (1.0 mmol, 2.0 mmol, 4.0 mmol) of triethylamine (TEA) were added slowly with uniform stirring, and a white precipitate was generated within 2 h at room temperature. Finally, organic amine TEA in Hie-Zn-MOF powders was easily removed by washing with DMF (10 mL × 2) and methanol (10 mL × 2), followed by vacuum drying at 80 °C for 12 h. The samples were denoted as Hie-Zn-MOF-TEA(*m*) (*m* is the addition dosage of TEA, *m* = 1.0, 2.0, and 4.0). With regard to the generality, other

organic amines of tripropylamine (TPA) or triamylamine (TAA) were also checked for the Hie-Zn-MOF synthesis. For the purpose of checking the function of organic amines in the Hie-Zn-MOF synthesis, Zn-MOF powders were obtained by continuous stirring for 1 week at room temperature without adding any organic amine keeping the other conditions all the same with Hie-Zn-MOF synthesis, denoted as Mic-Zn-MOF-RT. For the comparison on catalytic activity, the microporous Zn-MOF crystals were prepared *via* a solvothermal synthesis in our previous report¹⁷ and denoted as Mic-Zn-MOF-Sol.

Catalytic CO₂ cycloaddition reaction with epoxide

In a typical run of the catalytic experiment, a mixture of epoxide (34.5 mmol), Hie-Zn-MOF catalyst and Bu₄NBr cocatalyst was placed in a 50 mL stainless-steel autoclave. Then, CO₂ gas was imported slowly to expel the remaining air in the autoclave. At the target reaction temperature, the autoclave was filled with CO₂ to 1 MPa, and during the reaction the pressure was maintained at 1 MPa by adding CO₂. Upon completion, the autoclave was cooled to 0 °C and the residual CO₂ was discharged slowly. The mixture was extracted by ethyl acetate and determined on GC analysis, finally, the Hie-Zn-MOF catalyst was separated *via* simple centrifugation, washed three times with ethyl acetate (5 mL × 3), dried at 60 °C for 12 h and used for the next run.

Conflicts of interest

There are no conflicts to declare.

Acknowledgements

Thanks for the financial support from National Natural Science Foundation of China (21972034), the State Key Lab of Urban Water Resource and Environment of Harbin Institute of Technology (HIT2019DX12).

Notes and references

- 1 M. S. Liu, X. Wang, Y. C. Jiang, J. M. Sun and M. Arai, Hydrogen Bond Activation Strategy for Cyclic Carbonates Synthesis from Epoxides and CO₂: Current State of the Art of Catalyst Development and Reaction Analysis, *Catal. Rev.*, 2019, **61**(2), 214–269.
- 2 J. Liang, R. P. Chen, X. Y. Wang, T. T. Liu, X. S. Wang, Y. B. Huang and R. Cao, Postsynthetic Ionization of an Imidazole-Containing Metal-Organic Framework for the Cycloaddition of Carbon Dioxide and Epoxides, *Chem. Sci.*, 2017, **8**(2), 1570–1575.
- 3 J. Zhu, J. Liu, Y. Machain, B. Bonnett, S. Lin, M. Cai, M. C. Kessinger, P. M. Usov, W. Xu, S. D. Senanayake, D. Troya, A. R. Esker and A. J. Morris, Insights into CO₂ Adsorption and Chemical Fixation Properties of VPI-100

- Metal-Organic Frameworks, *J. Mater. Chem. A*, 2018, **6**(44), 22195–22203.
- 4 C. I. Ezugwu, N. A. Kabir, M. Yusubov and F. Verpoort, Metal-Organic Frameworks Containing N-Heterocyclic Carbenes and Their Precursors, *Coord. Chem. Rev.*, 2016, **307**, 188–210.
- 5 S. Zhang, K. Dokko and M. Watanabe, Porous Ionic Liquids: Synthesis and Application, *Chem. Sci.*, 2015, **6**(7), 3684–3691.
- 6 J. W. Maina, C. Pozo-Gonzalo, L. Kong, J. Schütz, M. Hill and L. F. Dumée, Metal Organic Framework Based Catalysts for CO₂ Conversion, *Mater. Horiz.*, 2017, **4**(3), 345–361.
- 7 J. Koo, I. C. Hwang, X. Yu, S. Saha and K. Kim, Hollowing out MOFs: Hierarchical Micro- and Mesoporous MOFs with Tailorable Porosity via Selective Acid Etching, *Chem. Sci.*, 2017, **8**(10), 6799–6803.
- 8 L. F. Song, J. Zhang, L. X. Sun, F. Xu, F. Li, H. Z. Zhang, X. L. Si, C. L. Jiao, Z. B. Li, S. Liu, Y. L. Liu, H. Y. Zhou, D. L. Sun, Y. Du, Z. Cao and Z. Gabelica, Mesoporous Metal-Organic Frameworks: Design and Applications, *Energy Environ. Sci.*, 2012, **5**, 7508–7520.
- 9 M. H. Beyzavi, R. C. Klet, S. Tussupbayev, J. Borycz, N. A. Vermeulen, C. J. Cramer, J. F. Stoddart, J. T. Hupp and O. K. Farha, A Hafnium-Based Metal-Organic Framework as an Efficient and Multifunctional Catalyst for Facile CO₂ Fixation and Regioselective and Enantioselective Epoxide Activation, *J. Am. Chem. Soc.*, 2014, **136**(45), 15861–15864.
- 10 S. Wu, X. Xing, D. Wang, J. Zhang, J. Chu, C. Yu, Z. Wei, M. Hu, X. Zhang and Z. Li, Highly Ordered Hierarchically Macroporous MIL-125 with High Specific Surface Area for Photocatalytic CO₂ Fixation, *ACS Sustainable Chem. Eng.*, 2019, **8**(1), 148–153.
- 11 W. Liang, L. Li, J. Hou, N. D. Shepherd, T. D. Bennett, D. M. D'Alessandro and V. Chen, Linking Defects, Hierarchical Porosity Generation and Desalination Performance in Metal-Organic Frameworks, *Chem. Sci.*, 2018, **9**(14), 3508–3516.
- 12 R. Babu, A. C. Kathalikkattil, R. Roshan, J. Tharun, D. W. Kim and D.-W. Park, Dual-Porous Metal Organic Framework for Room Temperature CO₂ Fixation via Cyclic Carbonate Synthesis, *Green Chem.*, 2016, **18**(1), 232–242.
- 13 J. F. Kurisingal, Y. Rachuri, Y. Gu, Y. Choe and D. W. Park, Multi-Variate Metal Organic Framework as Efficient Catalyst for the Cycloaddition of CO₂ and Epoxides in a Gas-Liquid-Solid Reactor, *Chem. Eng. J.*, 2020, 386–396.
- 14 N. Stock and S. Biswas, Synthesis of Metal-Organic Frameworks (MOFs): Routes to Various MOF Topologies, Morphologies, and Composites, *Chem. Rev.*, 2012, **112**(2), 933–969.
- 15 L. F. Chen, Y. Lu, L. Yu and X. W. Lou, Designed Formation of Hollow Particle-Based Nitrogen-Doped Carbon Nanofibers for High-Performance Supercapacitors, *Energy Environ. Sci.*, 2017, **10**(8), 1777–1783.
- 16 M. Wang, J. Liu, C. Guo, X. Gao, C. Gong, Y. Wang, B. Liu, X. Li, G. G. Gurzadyan and L. Sun, Metal-Organic Frameworks (ZIF-67) as Efficient Cocatalysts for Photocatalytic Reduction of CO₂: The Role of the Morphology Effect, *J. Mater. Chem. A*, 2018, **6**(11), 4768–4775.
- 17 J. W. Lan, M. S. Liu, X. Lu, X. Zhang and J. M. Sun, Novel 3D Nitrogen-Rich Metal Organic Framework for Highly Efficient CO₂ Adsorption and Catalytic Conversion to Cyclic Carbonates under Ambient Temperature, *ACS Sustainable Chem. Eng.*, 2018, **6**(7), 8727–8735.
- 18 S. Laha, D. Rambabu, S. Bhattacharyya and T. K. Maji, Modulating Hierarchical Micro/Mesoporosity by a Mixed Solvent Approach in Al-MOF: Stabilization of MAPBB₃ Quantum Dots, *Chem. – Eur. J.*, 2020, 1–10.
- 19 D. A. Yang, H. Y. Cho, J. Kim, S. T. Yang and W. S. Ahn, CO₂ Capture and Conversion Using Mg-MOF-74 Prepared by a Sonochemical Method, *Energy Environ. Sci.*, 2012, **5**, 6465–6473.
- 20 L. Tang, S. Zhang, Q. Wu, X. Wang, H. Wu and Z. Jiang, Heterobimetallic Metal-Organic Framework Nanocages as Highly Efficient Catalysts for CO₂ conversion under Mild Conditions, *J. Mater. Chem. A*, 2018, **6**(7), 2964–2973.
- 21 J. Liao, W. Zeng, B. Zheng, X. Cao, Z. Wang, G. Wang and Q. Yang, Highly Efficient CO₂ Capture and Conversion of a Microporous Acylamide Functionalized Rht-Type Metal-Organic Framework, *Inorg. Chem. Front.*, 2020, **7**(9), 1939–1948.
- 22 H. F. Zhou, B. Liu, L. Hou, W. Y. Zhang and Y. Y. Wang, Rational Construction of a Stable Zn₄O-Based MOF for Highly Efficient CO₂ Capture and Conversion, *Chem. Commun.*, 2018, **54**(5), 456–459.
- 23 D. Ma, K. Liu, J. Li and Z. Shi, Bifunctional Metal-Free Porous Organic Framework Heterogeneous Catalyst for Efficient CO₂ Conversion under Mild and Cocatalyst-Free Conditions, *ACS Sustainable Chem. Eng.*, 2018, **6**(11), 15050–15055.
- 24 Z. Y. Gao, X. Zhang, P. Xu and J. M. Sun, Dual Hydrogen-Bond Donor Group-Containing Zn-MOF for the Highly Effective Coupling of CO₂ and Epoxides under Mild and Solvent-Free Conditions, *Inorg. Chem. Front.*, 2020, **7**(10), 1995–2005.
- 25 P. Cui, Y. G. Ma, H. H. Li, B. Zhao, J. R. Li, P. Cheng, P. B. Balbuena and H. C. Zhou, Multipoint Interactions Enhanced CO₂ Uptake: A Zeolite-like Zinc-tetrazole Framework with 24-nuclear Zinc Cages, *J. Am. Chem. Soc.*, 2012, **134**, 18892–18895.
- 26 X. Guan, G. Chen and C. Shang, ATR-FTIR and XPS Study on the Structure of Complexes Formed Upon the Adsorption of Simple Organic Acids on Aluminum Hydroxide, *J. Environ. Sci.*, 2007, **19**(4), 438–443.
- 27 Z. Zhang, L. Pfefferle and G. L. Haller, Comparing Characterization of Functionalized Multi-Walled Carbon Nanotubes by Potentiometric Proton Titration, NEXAFS, and XPS, *Chin. J. Catal.*, 2014, **35**(6), 856–863.

- 28 Z. F. Xin, X. S. Chen, Q. Wang, Q. Chen and Q. F. Zhang, Nanopolyhedrons and Mesoporous Supra-Structures of Zeolitic Imidazolate Framework with High Adsorption Performance, *Microporous Mesoporous Mater.*, 2013, **169**(15), 218–221.
- 29 J. Cravillon, C. A. Schroder, R. Nayuk, J. Gummel, K. Huber and M. Wiebcke, Fast Nucleation and Growth of ZIF-8 Nanocrystals Monitored by Time-Resolved *In Situ* Small-Angle and Wide-Angle X-Ray Scattering, *Angew. Chem., Int. Ed.*, 2011, **50**(35), 8067–8071.
- 30 D.-A. Yang, H.-Y. Cho, J. Kim, S.-T. Yang and W.-S. Ahn, CO₂ capture and Conversion Using Mg-MOF-74 Prepared by a Sonochemical Method, *Energy Environ. Sci.*, 2012, **5**(4), 6465–6473.
- 31 C. Duan, F. Li, J. Xiao, Z. Liu, C. Li and H. Xi, Rapid Room-Temperature Synthesis of Hierarchical Porous Zeolitic Imidazolate Frameworks with High Space-Time Yield, *Sci. China Mater.*, 2017, **60**(12), 1205–1214.
- 32 X. Chen, X. Jiang, C. Yin, B. Zhang and Q. Zhang, Facile Fabrication of Hierarchical Porous ZIF-8 for Enhanced Adsorption of Antibiotics, *J. Hazard. Mater.*, 2019, **367**, 194–204.
- 33 X. Zhang, C. Y. Chuah, P. Dong, Y. H. Cha, T. H. Bae and M. K. Song, Hierarchically Porous Co-MOF-74 Hollow Nanorods for Enhanced Dynamic CO₂ Separation, *ACS Appl. Mater. Interfaces*, 2018, **10**(50), 43316–43322.
- 34 R. Babu, R. Roshan, A. C. Kathalikkattil, D. W. Kim and D. W. Park, Rapid, Microwave-Assisted Synthesis of Cubic, Three-Dimensional, Highly Porous MOF-205 for Room Temperature CO₂ Fixation via Cyclic Carbonate Synthesis, *ACS Appl. Mater. Interfaces*, 2016, **8**(49), 33723–33731.
- 35 Y. F. Wu, X. H. Song, S. Li, J. H. Zhang, X. H. Yang, P. X. Shen, J. Li, J. Gao, R. P. Wei, J. Zhang and G. M. Xiao, 3D-Monoclinic M-BTC MOF (M=Mn, Co, Ni) as Highly Efficient Catalysts for Chemical Fixation of CO₂ into Cyclic Carbonates, *J. Ind. Eng. Chem.*, 2018, **58**, 296–303.
- 36 H. M. He, Q. Q. Zhu, J. N. Zhao, H. M. Sun, J. Chen, C. P. Li and M. Du, Rational, Construction of an Exceptionally Stable MOF Catalyst with Metal-Adeninate Vertices toward CO₂ Cycloaddition under Mild and Cocatalyst-Free Conditions, *Chem. – Eur. J.*, 2019, **25**, 11474–11480.
- 37 D. Shao, J. B. Shi, J. L. Zhang, X. N. Tan, T. Luo, X. Y. Cheng, B. X. Zhang and B. X. Han, Solvent Impedes CO₂ Cycloaddition on Metal-Organic Frameworks, *Chem. – Asian J.*, 2018, **13**(4), 386–389.
- 38 A. K. Kathalikkattil, D. W. Kim, J. Tharun, H. G. Soek, R. Roshana and D. W. Park, Aqueous Microwave Synthesized Carboxyl Functional Molecular Ribbon Coordination Framework Catalyst for the Synthesis of Cyclic Carbonates from Epoxides and CO₂, *Green Chem.*, 2014, **16**, 1607–1616.
- 39 Y. Rachuri, J. F. Kurisingal, R. K. Chitumalla, S. Vuppala, Y. G. Gu, J. Jang, Y. Choe, E. Suresh and D. W. Park, Adenine-Based Zn(II)/Cd(II) Metal-Organic Frameworks as Efficient Heterogeneous Catalysts for Facile CO₂ Fixation into Cyclic Carbonates: A DFT-Supported Study of the Reaction Mechanism, *Inorg. Chem.*, 2019, **58**(17), 11389–11403.
- 40 Y. X. Li, X. Zhang, J. W. Lan, P. Xu and J. M. Sun, Porous Zn(Bmic)(AT) MOF with Abundant Amino Groups and Open Metal Sites for Efficient Capture and Transformation of CO₂, *Inorg. Chem.*, 2019, **58**(20), 13917–13926.
- 41 J. F. Kurisingal, Y. Rachuri, Y. Gu, Y. Choe and D. W. Park, Fabrication of Hierarchically Porous MIL-88-NH₂(Fe): a Highly Efficient Catalyst for the Chemical Fixation of CO₂ under Ambient Pressure, *Inorg. Chem. Front.*, 2019, **6**(12), 3613–3620.
- 42 W. Meng, Y. Zeng, Z. Liang, W. Guo, C. Zhi, Y. Wu, R. Zhong, C. Qu and R. Zou, Tuning Expanded Pores in Metal-Organic Frameworks for Selective Capture and Catalytic Conversion of Carbon Dioxide, *ChemSusChem*, 2018, **11**(21), 3751–3757.
- 43 J. B. DeCoste, J. A. Rossin and G. W. Peterson, Hierarchical Pore Development by Plasma Etching of Zr-Based Metal-Organic Frameworks, *Chemistry*, 2015, **21**(50), 18029–18032.
- 44 R. Das, S. S. Dhankhar and C. M. Nagaraja, Construction of a Bifunctional Zn(II)-Organic Framework Containing a Basic Amine Functionality for Selective Capture and Room Temperature Fixation of CO₂, *Inorg. Chem. Front.*, 2020, **7**(1), 72–81.